Biophysical Journal Volume 101 November 2011 2417–2425

Measurement of Lipid Nanodomain (Raft) Formation and Size in Sphingomyelin/POPC/Cholesterol Vesicles Shows TX-100 and Transmembrane Helices Increase Domain Size by Coalescing Preexisting Nanodomains But Do Not Induce Domain Formation

Priyadarshini Pathak and Erwin London*
Department of Biochemistry and Cell Biology, Stony Brook University, Stony Brook, New York

ABSTRACT Mixtures of unsaturated lipids, sphingolipids, and cholesterol form coexisting liquid-disordered and sphingolipid and cholesterol-rich liquid-ordered (Lo) phases in water. The detergent Triton X-100 does not readily solubilize Lo domains, but does solubilize liquid-disordered domains, and is commonly used to prepare detergent-resistant membranes from cells and model membranes. However, it has been proposed that in membranes with mixtures of sphingomyelin (SM), 1-palmitoyl 2-oleoyl phosphatidylcholine (POPC), and cholesterol Triton X-100 may induce Lo domain formation, and therefore detergent-resistant membranes may not reflect the presence of preexisting domains. To examine this hypothesis, the effect of Triton on Lo domain formation was measured in SM/POPC/cholesterol vesicles. Nitroxide quenching methods that can detect ordered nanodomains with radii >12 Å showed that in the absence of Triton X-100 this mixture formed ordered state domains that melt with a midpoint (= T_{mid}) at ~45°C. However, T_{mid} was lower when detected using various fluorescence resonance energy transfer (FRET) pairs. Furthermore, the T_{mid} value was Ro dependent, and decreased as Ro increased. Because FRET can only readily detect domains with radii >Ro, this result can be explained by domain radii that are close to Ro and decrease as temperature increases. An analysis of FRET and quenching data suggests that nanodomain radius gradually decreases from ≥150 Å to <40 Å as temperature increases from 10 to 45°C. Interestingly, the presence of Triton X-100 or a transmembrane-type peptide did not stabilize ordered state formation when detected by nitroxide quenching, i.e., did not increase T_{mid}. However, FRET-detected T_{mid} did increase in the presence of Triton X-100 or a transmembrane peptide, indicating that both increased domain size. Controls showed that the results could not be accounted for by probe-induced perturbations. Thus, SM/POPC/cholesterol, a mixture similar to that in the outer leaflet of plasma membranes, forms nanodomains at physiological temperatures, and TX-100 does not induce domain formation or increase the fraction of the bilayer in the ordered state, although it does increase domain size by coalescing preexisting domains.

INTRODUCTION

The formation of membrane lipid domains (rafts) in cells has received much attention because of its implications for membrane processes, including bacterial and viral infection, signal transduction, and sorting. Early studies speculated that sphingolipid microdomains played a role in sorting (1), and the observation that detergent-resistant membranes (DRMs) rich in sphingolipids (and cholesterol) could be isolated from cell membranes upon addition of Triton X-100 (TX-100) suggested that DRMs might correspond to cellular sphingolipid microdomains (2). The observation that sphingolipid and cholesterol (chol)-rich DRMs could be isolated from model membranes only under conditions in which spectroscopic methods showed preexisting liquid-ordered (Lo) domains were present, led to the hypothesis that DRMs might arise from cellular Lo domains (3,4).

Because addition of detergent to membrane-containing samples is a perturbation, there is concern that TX-100 could alter domain formation (5,6). However, in addition to the studies above, many subsequent studies have confirmed that when Lo and liquid-disordered (Ld) domains coexist, the DRMs arise from the Lo region of the membrane (7–11). On the other hand, it has been reported by one group that Lo domains in the mixture 1:1:1 sphingomyelin (SM), 1-palmitoyl 2-oleoyl phosphatidylcholine (POPC), and cholesterol (SM/POPC/chol) form at higher temperatures only in the presence of TX-100 (12,13), and this has been frequently cited as evidence that DRM may be a detergent artifact. In this study, we used spectroscopic methods to detect the presence and size of ordered domains as a function of temperature for SM/POPC/chol. This mixture was found to form nanodomains whose size decreased as temperature increased. The presence of TX-100 (or transmembrane helices) increased domain size without increasing the amount of the bilayer in an ordered state. These results have important implications for the reliability of TX-100 insolubility as a method to detect ordered domains.

MATERIALS AND METHODS

Materials

Porcine brain sphingomyelin (bSM), chicken egg sphingomyelin (eSM), 1-palmitoyl-2-oleoyl-phosphatidylcholine (POPC), chol, 1,2-dipalmitoylphosphatidylethanolamine-*N*-(7-nitro-2-1,3-benzoxadiazol-4-yl) (NBD-DPPE), 1,2-dipalmitoylphosphatidylethanolamine-*N*-(1-pyrenesulfonyl) ammonium

Submitted June 22, 2011, and accepted for publication August 30, 2011.
*Correspondence: erwin.london@stonybrook.edu
Editor: Thomas J. McIntosh.

0006-3495/11/11/2417/9 $2.00
doi: 10.1016/j.bpj.2011.08.059

salt (pyrene-DPPE), 1,2-dioleoylphosphoethanolamine-*N*-(Lissamine Rhodamine B Sulfonyl) (rhod-DOPE), and 1-palmitoyl-2-stearoyl-(10-doxyl)-phosphatidylcholine (10-SLPC) were purchased from Avanti Polar Lipids (Alabaster, AL). 1,6-diphenyl-1,3,5-hexatriene (DPH) and TEMPO were purchased from Sigma-Aldrich (St. Louis, MO). Acetyl-$K_2W_2L_8AL_8W_2K_2$-amide (LW peptide) was purchased from Anaspec (San Jose, CA) and used without further purification. TX-100 was purchased from Yorktown Research (Hackensack NJ). Lipids and probes were dissolved in chloroform (with the exception of DPH and TEMPO, which were dissolved in ethanol) and stored at −20°C. The concentrations of lipids were determined by dry weight and that of fluorescent molecules and LW peptide by absorbance using $\varepsilon_{\text{NBD-DPPE}}$ 21,000 $M^{-1}cm^{-1}$ at 460 nm, $\varepsilon_{\text{pyrene-DPPE}}$ 35,000 $M^{-1}cm^{-1}$ at 350 nm, $\varepsilon_{\text{rhod-DOPE}}$ 88,000 $M^{-1}cm^{-1}$ at 560 nm, ε_{DPH} 84,800 $M^{-1}cm^{-1}$ at 352 nm, and $\varepsilon_{\text{LW peptide}}$ 22,000 $M^{-1}cm^{-1}$ at 280 nm. High performance thin layer chromatography (TLC) plates (Silica Gel 60) were purchased from VWR International (Batavia, IL).

Vesicle preparation

Multilamellar vesicles (MLVs) and ethanol dilution small unilamellar vesicles (SUVs) were prepared similar to as described previously (14). For SUVs, lipids and fluorophores were pipetted into glass tubes, dried under N_2, dissolved in 25 μL ethanol and dispersed in 975 μL phosphate buffered saline (PBS: 1 mM KH_2PO_4, 10 mM Na_2HPO_4, 137 mM NaCl, and 2.7 mM KCl, pH 7.4). For preparing MLV, the dried lipid was redissolved in 20 μL chloroform, redried under N_2 followed by drying under high vacuum for 2 h, and dispersal in 70°C PBS pH 7.4. Final samples contained 500 μM lipids. When present, TX-100 and LW peptide were pipetted along with lipids. Background samples lacking fluorescent probe were also prepared. Large unilamellar vesicles (LUVs) were prepared by subjecting MLVs to 5 cycles of freeze/thaw, alternately placing the sample in a dry ice/acetone bath and room temperature water bath. The vesicles were then passed (11 cycles) through a mini-extruder (Avanti Polar Lipids) using 1000 Å filters to obtain LUVs. For fluorescence resonance energy transfer (FRET) measurements, LUVs were prepared only by extrusion (without freeze/thawing, which was found to segregate FRET probes into different vesicles). All samples were incubated at room temperature for 1 h before initiating the fluorescence measurements.

Fluorescence and absorbance measurements

Fluorescence was measured on SPEX Fluorolog 3 spectrofluorometer (Jobin-Yvon, Edison, NJ) using quartz semimicro cuvettes (excitation path length 10 mm and emission path length 4 mm). DPH fluorescence was measured at an excitation λ of 358 nm and emission λ of 430 nm. NBD fluorescence was measured at an excitation λ of 460 nm and an emission λ of 534 nm. Pyrene fluorescence was measured at an excitation λ of 350 nm and an emission λ of 379 nm. TX-100 fluorescence was measured at an excitation λ of 260 nm and emission λ of 310 nm. Slit-width bandwidths for fluorescence intensity measurements were set to 4 nm (2 mm physical size) for excitation and emission. The reported values were corrected for background fluorescence except for DPH fluorescence, where background values were <0.02% of the sample values. Absorbance was measured with Beckman 640 spectrophotometer (Beckman Instruments, Fullerton, CA) using quartz cuvettes.

Measurement of TX-100 binding to MLV and determination of lipid composition after TX-100 solubilization by high performance-TLC

The amount of vesicle-bound TX-100 was calculated as follows. 2 mL aliquots of MLV containing 500 μM bSM/POPC/chol (1:1:1) and TX-100 (150, 300, or 500 μM) were prepared as described previously, and then incubated at room temperature for 1 h. 1 mL aliquots were centrifuged at 14 000 rpm (11,000 × *g*) for 20 min. in an Eppendorf 5415C tabletop centrifuge; the supernatant was separated from the pellet and the pellet was resuspended in 1 mL PBS pH 7.4. 250 μL aliquots each of MLV before centrifugation, supernatant, and resuspended pellet were then diluted to 1 mL with 750 μL PBS pH 7.4, and fluorescence measured. Controls showed no loss of TX-100 during vesicle preparation (e.g., due to sublimation during the high vacuum step). The intensity of TX-100 fluorescence per unit concentration was found to be insensitive to whether TX-100 concentration was above or below its critical micelle concentration or whether the TX-100 was bound to lipid or not (not shown). Lipids were analyzed by TLC as previously described (15). Details are given in the Supporting Material.

Measurement of the temperature dependence of DPH fluorescence quenching by TEMPO

The temperature dependence of TEMPO quenching was carried out as described in (14). SUVs and MLVs with 500 μM lipid and 0.1 mol % DPH were prepared as described previously. A 6.2 μL aliquot of a 322 mM stock solution of TEMPO dissolved in ethanol was added to the samples (defined as F samples) to obtain a final concentration of 2 mM unless otherwise stated. The same volume of ethanol was added to the samples that did not contain quencher (Fo samples). The samples were incubated at room temperature for 10 min, after which they were cooled to 16°C and the fluorescence measurements were initiated. Cuvette temperature was measured with a probe thermometer placed in the cuvette before each measurement (Fisher brand traceable digital thermometer with an YSI microprobe, Fisher Scientific). The cuvette temperature was increased at a rate of ~0.5°C per min and readings were taken every 4°C. The ratio of the average fluorescence intensity in the presence of quencher to its absence (F/Fo) was calculated. Background fluorescence measurements were taken at 16 and 60°C. The backgrounds were not subtracted because they were <0.02% of the DPH fluorescence signal. The melting midpoint temperature (T_{mid}) was calculated for each curve. T_{mid} was defined as a point of maximum slope of a sigmoidal fit of F/Fo data. (Slide Write Plus software, Advanced Graphics Software, Encinitas, CA).

Measurement of the temperature dependence of fluorescence anisotropy

DPH fluorescence anisotropy measurements were made using a SPEX automated Glan-Thompson polarizer accessory with slit-width band-widths set to 4.2 nm (excitation) and 8.4 nm (emission). Anisotropy values were calculated as described previously (14). Anisotropy as a function of temperature was measured for MLV samples containing 0.1 mol % DPH and 500 μM lipid, prepared as described previously. The samples were incubated at room temperature for 1 h and then cooled to 16°C. Samples were then heated in steps of 4°C and anisotropy was measured at each step once the temperature stabilized.

Measurement of the temperature dependence of FRET

Förster resonance energy transfer using donor acceptor pairs with different Förster radii (Ro) was measured in MLV prepared as described previously. Unless otherwise noted vesicles contained 0.1 mol % (for NBD-DPPE and DPH) or 0.05 mol % (for pyrene-DPPE) donor and 2 mol % acceptor (rhod-DOPE) in F samples. The Fo samples contained only donor. Background samples for Fo (containing only lipid and lacking donor) and for F (containing lipid plus acceptor) samples were also prepared. Samples were prepared at 70°C and then incubated at room temperature for 1 h, after which they were cooled to 16°C and the fluorescence measurements initiated. Cuvette

temperature, measured as described previously, was increased at a rate of ~0.5°C per min. and readings were taken every 4°C. In addition, background fluorescence at 16 and 64°C was measured, averaged for the two temperatures (as backgrounds were found to be independent of temperature), and then subtracted from the FRET sample values. The ratio of fluorescence intensity in the presence of acceptor to its absence (F/Fo) was calculated. The domain detection midpoint temperature (T_{mid}) was calculated for each curve. T_{mid} was defined as a point of maximum slope of a sigmoidal fit of F/Fo data. The maximum temperature at which there is facile detection of Lo domains by FRET (T_{upper}) was calculated from the intersection of a line fit to F/Fo at T_{mid}, and the 2 F/Fo points closest above and 2 below T_{mid} and the line F/Fo = F/Fo value at the upper limit of the sigmoidal fit to F/Fo versus temperature. (Due to their temperature dependence in the Ld state, T_{upper} could not be calculated for TEMPO quenching and anisotropy.)

RESULTS

Stability of ordered state in 1:1:1 bSM/POPC/chol vesicles: neither TX-100 nor a transmembrane peptide stabilize ordered state formation

First, quenching of DPH fluorescence by TEMPO was measured (14,16). TEMPO is a nitroxide-bearing molecule that binds to Ld domains more strongly than to Lo domains (14,17), so in bilayers partly or wholly in an ordered state quenching of DPH, which partitions evenly between ordered and disordered domains (3,18), by TEMPO is weak, but when a bilayer is fully in the Ld state, quenching is strong (14). By measuring the temperature dependence of quenching the midpoint melting temperature (T_{mid}) of Lo domains can be determined (14). The T_{mid} value, given by the inflection point in the quenching curve, represents the point at which the slope of the curve, and thus the decrease in membrane order as a function of temperature, is a maximum. (It is not necessarily the point at which the membrane is 50% in the Lo state.) The higher the T_{mid} value, the greater the stability of ordered domains (14). Fig. 1 *A* (*circles*) shows the temperature dependence of TEMPO quenching in MLVs composed of a 1:1:1 (mol/mol) mixture of bSM/POPC/chol. There is a sigmoidal dependence of normalized DPH fluorescence (= F/Fo, the fraction of unquenched fluorescence) upon temperature, with quenching levels in good agreement with recent studies on similar mixtures (14). The T_{mid} value occurs at ~45°C (Table 1). Controls in which TEMPO concentration was varied show that TEMPO binding to vesicles did not alter T_{mid} values up to 2 mM (Fig. S1 in the Supporting Material).

A similar DPH quenching curve, with perhaps a small decrease in T_{mid} was observed in 1:1:1 bSM/POPC/chol when lipids were mixed with TX-100 before vesicle formation (final TX-100 concentration 150 μM) (Table 1 and Fig. 1 *A*, *solid triangles*). There was very little if any additional dependence of T_{mid} upon increasing TX-100 concentration up to severalfold above the critical micelle concentration of TX-100 (~200–300 μM (19)) (Fig. S2 and Table 1). The presence in the vesicles of 0.45 mol % of LW peptide, a Leu-rich transmembrane-type peptide

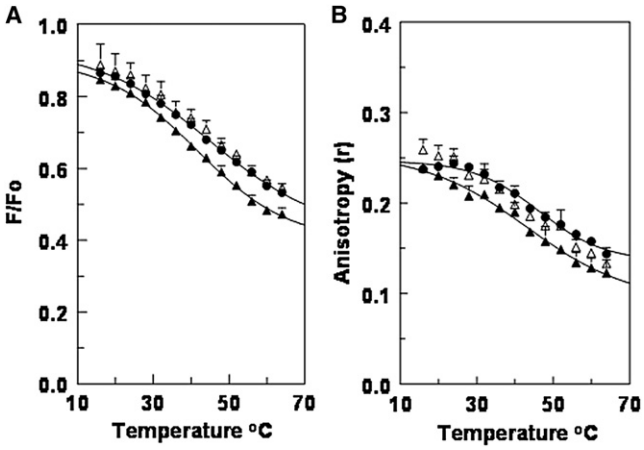

FIGURE 1 Ordered domain thermal stability in lipid vesicles and how it is affected by TX-100 and transmembrane peptide as measured by (*A*) quenching of DPH fluorescence by TEMPO and (*B*) DPH fluorescence anisotropy. In *A*, MLV were composed of 0.1 mol % DPH and 500 μM 1:1:1 (mol/mol) bSM/POPC/chol. Samples contained lipid only (*solid circles*, average of 6), lipid plus 150 μM TX-100 (*solid triangles*, average of 3), or lipid plus 0.45 mol % (2.25 μM) LW peptide (*open triangles*, average of duplicates). In addition, F samples contained 2 mM TEMPO. F/Fo is the ratio of fluorescence in the presence of TEMPO to that in the absence of TEMPO. (*B*) MLV were composed of 0.1 mol % DPH and 500 μM 1:1:1 (mol/mol) bSM/POPC/chol. Samples contained: lipid alone (*solid circles*, average of 6), lipid plus 150 μM TX-100 (*solid triangles*, average of 4), or lipid plus 0.45 mol % LW peptide (*open triangles*, average of 4). The error bars in this and the following figures are standard deviations, or if $n = 2$ range. Where error bars are not shown, they were too small to be displayed.

that partitions strongly into Ld domains (20) also had little, if any, effect upon T_{mid} (Table 1 and Fig. 1 *A*, *open triangles*).

Other experiments showed that the temperature-dependent change in quenching was reversible (Fig. S3 *A*), and that similar T_{mid} values with and without TX-100 were observed using LUVs or SUVs in place of MLV (Table S1).

To confirm results obtained from TEMPO quenching, the thermal stability of ordered state formed by 1:1:1 bSM/POPC/chol was measured using steady-state DPH fluorescence anisotropy (Fig. 1 *B*). The anisotropy of DPH fluorescence is high when it is in the Lo state, and decreases in the Ld state (14,21). Anisotropy in 1:1:1 bSM/POPC/chol at low temperature (*solid circles*) was equal to those previously observed for a mixture of Lo and Ld states, whereas the values at high temperature corresponded to those in an Ld state (14). As in the case of TEMPO quenching, there was a sigmoidal dependence upon temperature, with estimated T_{mid} values very similar to that measured with TEMPO quenching (Table 1). Samples containing 1:1:1 bSM/POPC/chol plus TX-100 (Fig. 1 *B*, s*olid triangles*) also exhibited a slight decrease in T_{mid} value similar to that determined by TEMPO quenching (Fig. 1 *B* and Table 1). As in the case of TEMPO quenching higher TX-100 concentrations did not greatly affect T_{mid} (Fig. S4 and Table 1). Samples containing membrane-inserted LW

TABLE 1 Ordered domain melting/detection temperatures under different conditions

Method donor/fluorophore	Acceptor/quencher	T_{mid} [T_{upper}, estimated] (°C)			
		Lipid alone	+TX-100 (150 μM)	+TX-100 (500 μM)	+LW peptide (0.45 mol %)
Quenching DPH	TEMPO	46.9 ± 3.4 (6)	41.6 ± 1.4 (3)	43.3 ± 0.5 (6)	46.1 ± 3.7 (2)
Anisotropy DPH		46.3 ± 1.9 (6)	41.0 ± 4.4 (4)	39.0 ± 3.6 (3)	40.9 ± 2.8 (4)
Quenching DPH	10-SLPC	47.1 ± 6.4 (4) [~69]	34.4 ± 2.7 (4) [~56]	nd	34.1 ± 2.4 (4) [~62]
FRET NBD-DPPE	rhod-DOPE	9.3 ± 0.3 (4) [~29]	25.7 ± 0.3 (4) [~40]	nd	23.4 ± 0.6 (4) [~37]
FRET DPH	rhod-DOPE	21.4 ± 0.1 (2) [~34]	33.1 ± 0.4 (2) [~52]	nd	30.8 ± 0.2 (2) [~49]
FRET pyrene-DPPE	rhod-DOPE	25.4 ± 0.5 (6) [~36]	35.3 ± 3.5 (4) [~56]	nd	31.4 ± 0.4 (4) [~46]

MLV samples were composed of 500 μM 1:1:1 (mol/mol) bSM:POPC:chol. T_{mid} for anisotropy and short-range quenching is the point at which %melting/°C is a maximum. T_{mid} for FRET is the temperature at which the change in F/Fo versus temperature is a maximum. T_{upper} is the maximum temperature at which there is facile detection of Lo domains. Calculation of T_{mid} and T_{upper} is described in Methods. Average T_{mid} and T_{upper} values in the presence and absence of TX-100 or transmembrane (LW) peptide are shown. Sample number is shown in parenthesis. Samples with 10-SLPC also contained 2 mol % DOPE. Error bars are SD when $n \geq 3$, and range if $n = 2$. nd = not determined.

peptide (Fig. 1 *B* and Table 1, *open triangles*) showed a slight decrease in T_{mid}.

Membrane composition in the presence of TX-100

To evaluate the effect (or lack of effect) of TX-100 on T_{mid}, it was important to determine how much TX-100 was bound to membranes. Both the amount of TX-100 bound to vesicles and the degree to which it solubilized vesicular lipids could influence T_{mid}. As shown in Table 2, the amount of bound TX-100 varied from ~4 mol % of the lipid at 150 μM TX-100 to ~10 mol % of total lipid in 500 μM TX-100. Lipid solubilization at different TX-100 concentrations was also measured. As shown in Table 2, most of the lipid was not solubilized by TX-100 at any of the concentrations tested. However, a significant amount of POPC was solubilized at 300 μM and especially at 500 μM TX-100. This lipid selectivity is expected because TX-100 selectively dissolves the lipids that are within Ld domains, which should be predominantly composed of POPC.

Segregation-detected nanodomain formation and size

The methods used above measure membrane order. To more directly probe lipid segregation into separate domains, methods dependent on lipid segregation were used. First, domain formation was detected by nitroxide-quenching using DPH as the fluorophore and the phospholipid 10-SLPC, which contains a nitroxide-bearing doxyl ring in the middle of one fatty acyl chain, as quencher. Unlike TEMPO quenching, which is strongly dependent upon TEMPO binding to membranes, and thus lipid packing, quenching by a nitroxide-labeled lipid directly detects lipid segregation (3). The doxyl group imparts a strong tendency to form and incorporate into Ld domains (3,20,22). The effective quenching range for nitroxides (Rc) is generally close to 12 Å (23). T_{mid} detected by 10-SLPC quenching was similar to that obtained by TEMPO quenching (Fig. 2 and Table 1). In general, TX-100 and LW peptide slightly decreased T_{mid}, similar to what was measured by TEMPO quenching and anisotropy (Table 1).

TABLE 2 Lipid and TX-100 composition of vesicles at different TX-100 concentrations

Triton X-100 (μM)	% Triton fluorescence in pellet	Triton bound	% SM in pellet	% Chol in pellet	% POPC in pellet
0	0	0	95.8	92.9	95.2
150	13.7 ± 0.6 (4)	21 μM	96.4	91.9	96.4
300	17.7 ± 0.4 (5)	53 μM	87.6	89.3	77.5
500	11.6 ± 0.5 (5)	58 μM	86.1	91.1	56.2

Total lipid concentration was 500 μM of 1:1:1 bSM:POPC:chol before solubilization. Error bars are SD (Triton X-100 fluorescence intensity was not affected by binding to vesicles (not shown)).

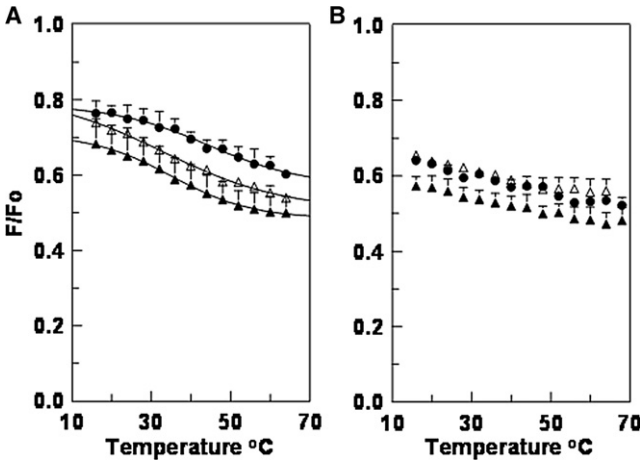

FIGURE 2 Effect of TX-100 and transmembrane peptide on detection of ordered domains assayed by quenching of DPH fluorescence by 10-SLPC. Samples were composed of MLV containing 0.1 mol % DPH and 500 μM lipid. (*A*) Fo samples contained 1:1:1 bSM/POPC/chol and F samples contained 7:(6:1):7 of bSM/(POPC/10-SLPC)/chol (= 4.8 mol % 10-SLPC). (*B*) Samples lacking SM. Fo samples contained 2:1 POPC/chol and F samples contained (POPC/10-SLPC)/chol in the ratio (6:1):3.5 (= 4.8 mol % 10-SLPC). All samples also contained 2 mol % DOPE. Samples contained: lipid only (*circles*), lipid plus 150 μM TX-100 (*solid triangles*), or lipid plus 0.45 mol % LW peptide (*open triangles*). The number of samples was four in each case shown.

Another method commonly used to detect domain formation is FRET. When a membrane has coexisting ordered and disordered domains, the segregation of donor and acceptor with different affinities for ordered and disordered domains results in a decrease in FRET, which is detected as an increase in normalized donor fluorescence (F/Fo). For measuring FRET, the acceptor used was rhod-DOPE, which partitions strongly into Ld domains (24). Donors with a significant affinity for ordered domains, NBD-DPPE, DPH, and pyrene-DPPE were used. Their FRET to rhod-DOPE has an effective Ro of 49 Å, 36 Å, and 26 Å, respectively, as determined from experimental measurements in homogeneous bilayers (Table S2).

The dependence of FRET upon temperature showed patterns very different from those measured by nitroxide quenching. Fig. 3 *A* (*circles*) shows that in bSM/POPC/chol vesicles when the donor was NBD-DPPE, FRET was strong throughout the range 10–60°C. Domains were only barely detected at low temperature, as shown by the weaker FRET (higher F/Fo) below 30°C. For FRET, T_{mid} is the temperature at which the change in FRET versus temperature is at a maximum. A crude T_{mid} value for domain detection is 9°C. In POPC/chol vesicles, which lack SM and form homogeneous bilayers FRET is very strong at all temperatures (Fig. 3 *B*). FRET curves were similar for 1:1:1 bSM:POPC:chol LUV samples, showing that the FRET and its temperature dependence were not greatly influenced by interbilayer FRET in MLV (Fig. S5 and Table S3). In contrast to samples lacking TX-100, domains could be easily detected for 1:1:1 bSM/POPC/chol vesicles in the presence of 150 μM TX-100 (in which TX-100 is mixed with the lipids before vesicle formation), which exhibited dramatically decreased FRET at lower temperatures (Fig. 3 *A*, *solid triangles*). The domains detected had an apparent T_{mid} ~25°C. The effect of TX-100 on FRET increased in a TX-100 dose-dependent fashion (Fig. S6).

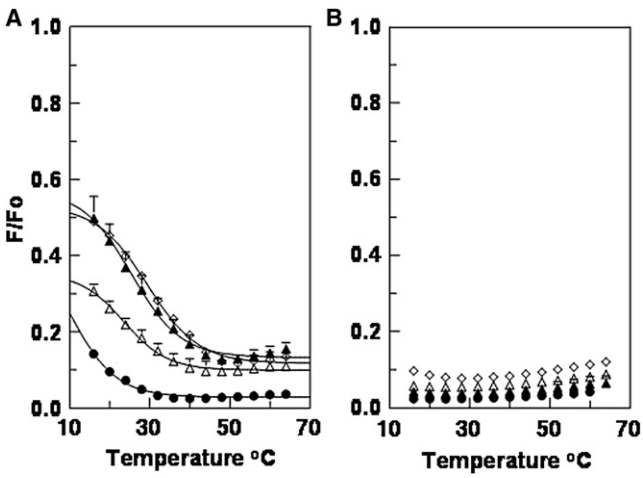

FIGURE 3 Detection of ordered domains by FRET and the effect of TX-100 and transmembrane peptide on domain detection. Samples were composed of MLV containing 500 μM: (*A*) 1:1:1 bSM/POPC/chol,or (*B*) 2:1 POPC/chol. F samples contained also FRET donor (0.1 mol % NBD-DPPE) and FRET acceptor (2 mol % rhod-DOPE). Fo samples also contained only FRET donor (0.1 mol % NBD-DPPE). Samples contained: lipid only (*circles*, average of 4), lipid plus 150 μM TX-100 (*solid triangles*, average of 4), lipid plus 0.45 mol % LW peptide (*open triangles*, average of 4), or lipid plus both 150 μM TX-100 and 0.45 mol % LW peptide (*diamonds*, average of 3). The ratio of donor fluorescence in the presence of acceptor to that in its absence (F/Fo) is graphed.

A decrease in FRET and increase in T_{mid} (to 23°C) was also observed in vesicles containing 0.45 mol % LW peptide (Fig. 3 *A*, *open triangles*). Samples containing both 0.45 mol % LW peptide and 150 μM TX-100 (*diamonds*) gave curves very similar to those with TX-100 alone (Fig. 3 *A*). POPC/chol vesicles showed no effect of TX-100 or LW peptide on FRET (Fig. 3 *B*).

Using NBD-DPPE to rhod-DOPE FRET samples containing 1:1:1 eSM/POPC/chol gave similar FRET results to those with brain SM, although domain formation in the absence of TX-100 was more easily detected at lower temperatures (Fig. S7).

At first glance, the observation that T_{mid} measured by FRET is lower than that measured by nitroxide quenching and anisotropy, and that there is a lack of FRET-detected domain formation in bSM/POPC/chol at temperatures at which they can be detected in the presence of TX-100 or LW peptide might seem to contradict conclusions of the nitroxide quenching and anisotropy results. How can FRET change so strongly in a temperature range in which the amount of ordered domains does not change? The likely explanation is that the domains formed in bSM/POPC/chol are too small to detect using the NBD-DPPE/rhod-DOPE FRET-pair under some conditions, and that TX-100 and LW peptide influence domain size. Nitroxide-induced quenching (which has a range of 12 Å (23)) and anisotropy are both very short-range processes that measure behavior of the lipid in which the probes are in direct contact, while NBD-to-rhod FRET is a longer range interaction, and requires that domain radius be greater than the interaction distance (i.e., Ro) in order to allow facile domain detection (see below).

To test the hypothesis that T_{mid} measured by FRET reflects domain size, and that domain size is altered by TX-100, FRET experiments were repeated with the DPH/rhod-DOPE (Fig. 4, *A* and *B*), and pyrene-DPPE/rhod-DOPE FRET pairs (Fig. 4, *C* and *D*), FRET pairs with smaller Ro values than the NBD-DPPE/rhod-DOPE pair. As predicted, without TX-100 domain formation (weakened FRET) could now be detected more easily in bSM/POPC/chol at lower temperatures, and the smaller the Ro, the higher the apparent T_{mid} for loss of Lo domain detection (Table 1). We also estimated the temperature (T_{upper}) that represents the upper limit of facile Lo domain detection (see Methods). A similar pattern was observed, in which the T_{upper} increased as Ro decreased. This progressive and Ro-dependent loss of domain detection as temperature increases indicates that domain size gradually decreases as

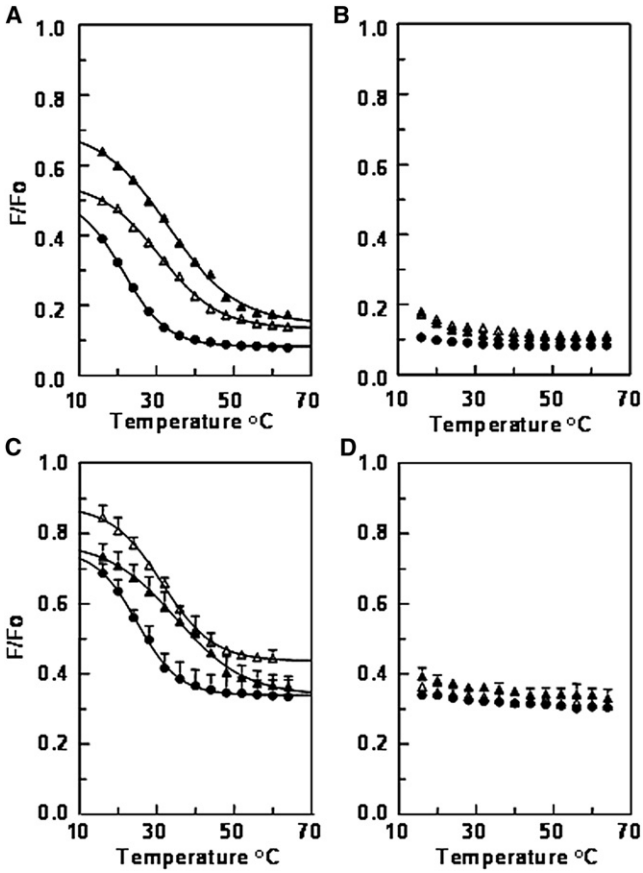

FIGURE 4 Effect of TX-100 and transmembrane peptide on ordered domain detection assayed by FRET pairs with shorter Ro than the NBD-rhodamine pair. Samples were composed of MLV containing 500 μM: (*A* and *C*) 1:1:1 bSM/POPC/chol or (*B* and *D*) 2:1 POPC/chol. In *A* and *B*, F samples also contained 0.1 mol % DPH as the FRET donor and 2 mol % rhod-DOPE as FRET acceptor. Fo samples also contained only 0.1 mol % DPH. Samples contained: lipid only (*circles*, average of duplicates), lipid plus 150 μM TX-100 (*solid triangles*, average of duplicates), or lipid plus 0.45 mol % LW peptide (*open triangles*, average of duplicates). In *C* and *D*, F samples contained as the FRET donor 0.05 mol % pyrene-DPPE and as the FRET acceptor 2 mol % rhod-DOPE. Fo samples contained only 0.05 mol % pyrene-DPPE. Samples contained lipid only (*circles*, average of 6), lipid plus 150 μM TX-100 (*solid triangles*, average of 4), or lipid plus 0.45 mol % LW peptide (*open triangles*, average of 4).The ratio of donor fluorescence in the presence of acceptor to that in its absence (F/Fo) is graphed.

temperature increases (see below). Furthermore, as in the case for T_{mid}, T_{upper} increased in the presence of TX-100 and LW peptide (Table 1).

In addition, the increase in apparent T_{mid} values in the presence of TX-100 or LW peptide when pyrene-DPPE and DPH were donors were smaller than when NBD-DPPE was the donor (Table 1). This is as expected if TX-100 and LW peptide only induce an increase in domain size, because for smaller Ro values FRET is less sensitive to domain size. (Also, notice that at low temperatures the difference between FRET levels with and without TX-100 is largest when NBD-DPPE is donor, smaller when DPH is donor, and smallest when pyrene-DPPE is donor.) Notice that even for these smaller Ro pairs, no evidence of domain formation was observed in POPC/chol vesicles, which form more homogeneous bilayers.

Using the DPH/rhod-DOPE pair, we also confirmed that thermal changes in FRET were reversible both in the presence and absence of TX-100 (Fig. S3 *B*).

It is unlikely that the results above reflect probe-induced perturbation of the lipid bilayers. For the FRET studies, a large perturbation of lipid melting due to donor is unlikely because the donors were used in very small amounts (1/2000 lipids for pyrene-DPPE and 1/1000 lipids for NBD-DPPE and DPH), and the same acceptor, rhod-DOPE and acceptor concentration was used. Thus, perturbation cannot explain the apparent differences in domain properties observed for different FRET pairs. A different issue is whether samples with the acceptor (2% rhod-DOPE), have different physical behavior than samples without acceptor; controls also show that this is unlikely. First, similar FRET results were obtained at 1 mol % rhod-DOPE (Fig. S8 and Table S3). Second, when DPH-10-SLPC quenching experiments were carried out both in the absence and presence of 2 mol % DOPE, no difference in quenching or its temperature dependence was observed (Fig. S9 and Table S3).

NBD-DOPE to rhod-DOPE FRET, and the effect of TX-100 upon FRET with this donor acceptor pair, was very similar in samples containing 4.7 mol % 10-SLPC and those lacking 10-SLPC (Fig. S10 and Table S3). This indicates that 10-SLPC did not greatly perturb domain formation or size. The conclusion that 10-SLPC did not perturb domain formation is further supported by the similarity of T_{mid} detected by 10-SLPC quenching to the T_{mid} values determined by TEMPO quenching and anisotropy (Table 1).

Combining FRET and 10-SLPC quenching results, it appears that TX-100, and LW peptides do not induce nanodomain formation, but do increase domain size. This means that in the presence of TX-100 and LW peptide there are larger Lo domains, but since the amount of the bilayer in the Lo state has not increased (as shown by TEMPO quenching, anisotropy, and 10-SLPC quenching) there must also be fewer of them.

Effect of cholesterol concentration upon FRET-detected nanodomain formation in the absence and presence of TX-100 or transmembrane peptide

In additional studies, the effect of chol concentration upon domain segregation in bSM/POPC/chol, both in the absence and presence of TX-100 and LW peptide was studied. As shown in Fig. 5, at room temperature for both the NBD-DPPE/rhod-DOPE FRET pair (Fig. 5 *A*) and the pyrene-DPPE/rhod-DOPE FRET pair (Fig. 5 *B*) domains could be detected by FRET at both medium and very high concentrations of chol. This is consistent with previous FRET studies

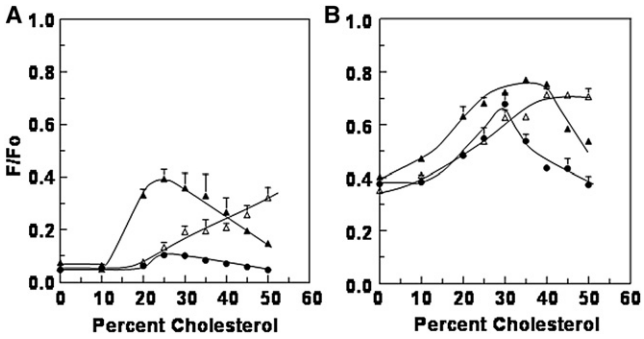

FIGURE 5 Effect of TX-100 and transmembrane peptide on FRET detection of domain formation as a function of chol concentration at room temperature. In *A*, donor: 0.1 mol % NBD-DPPE, acceptor: 2 mol % rhod-DOPE. (*B*) Donor: 0.05 mol % pyrene-DPPE, acceptor: 2 mol % rhod-DOPE. Samples were composed of MLV containing 500 μM 1:1:× bSM/POPC/chol. F samples also contained both FRET donor and acceptor. Fo samples also contained only FRET donor. The ratio of donor fluorescence in the presence of acceptor to that in its absence (F/Fo) is plotted versus chol concentration. (*A*) Samples contained: lipid (*circles*), lipid plus 150μM TX-100 (*solid triangles*, average of 3), or lipid plus 0.45 mol % LW peptide (*open triangles*, average of 4). (*B*) Samples contained lipid (*circles*, average of duplicates), lipid plus 150 μM TX-100 (*solid triangles*, average of duplicates), or lipid plus 0.45 mol % LW peptide (*open triangles*, average of duplicates).

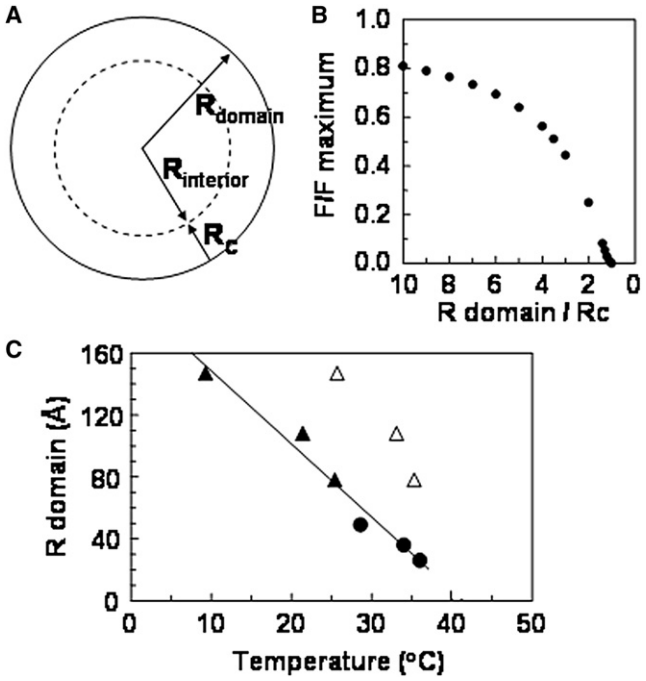

FIGURE 6 Schematic figure showing how FRET/quenching are affected by domain size. See the Supporting Material for calculations. (*A*) Illustration of interior zone in a circular domain. Rc, is the critical interaction distance (~Ro). R interior is the radius of the region in the domain largely protected from interaction with quenchers outside the domain. (*B*) The dependence of protection of a fluorescent group from quenchers outside of a domain upon domain radius. Protection is calculated for high enough quencher concentration to quench all fluorescence outside of domains and within Rc of the domain boundary. [(F/Fo)/(F maximum/ Fo)] = F/ F maximum = interior area of domain/total area of a domain = ratio of fluorescence arising within domains to that in domains approaching infinite size, at a constant fraction of membrane area within domains, i.e., when individual domain area decreases, domain number increases such that the fraction of bilayer area within domains is constant (see the Supporting Material). The change of F/F maximum versus R domain/Rc would be more gradual than shown for a quenching process with gradual distance dependence. (*C*) Lo domain size (Å) estimated using T_{mid} and T_{upper} values for different FRET pairs. Solid symbols, lipids alone, open symbols, lipids plus 150 μM TX-100. Triangles and circles show estimated radii of Lo domains at T_{mid} and T_{upper}, respectively. T_{upper} values $\geq$40°C were not included because above 35°C, FRET changes will reflect domain melting to a greater degree than changes in domain size. The linear fit shown is only to guide the eye.

showing that domain formation can occur at very high chol concentrations in a very similar mixture, SM/SOPC/chol (25).

There was a maximum degree of FRET-detected segregation near 25–35 mol % chol in both the absence and presence of TX-100. This suggests domain formation is either most stable, or domains are largest, at this chol concentration. In contrast, the effect of LW peptide upon FRET-detected segregation increased monotonically as chol concentration increased. These results indicate that the effects of TX-100 and a transmembrane helix upon domain properties are not restricted to values around 33 mol % chol, and that at high chol concentrations transmembrane helices have a stronger effect upon domain properties than TX-100. Even at very high chol (45 mol %), with TX-100 or LW peptide present FRET showed segregation persisted to above 37°C (Fig. S11).

Estimating nanodomain size

Calculating exact nanodomain size from FRET is difficult as FRET also depends upon acceptor concentration, partition of donor and acceptor between ordered and disordered domains, domain shape, and whether domains in the opposing leaflets are or are not in register. However, using multiple FRET/quencher pairs makes it possible to roughly estimate nanodomain size (Fig. 6). Processes such as FRET and nitroxide quenching have a distance dependence such that quenching is very strong only when fluorophore and quencher are within a critical distance (Rc) (Fig.6 *A*). Strong protection of a donor inside a domain from quenchers outside the domain requires a Lo domain radius greater than Rc. Crudely speaking, Rc~Ro (23).

As shown in Fig. 6 *B*, FRET basically cannot detect domains when domain radius is <Ro. Thus, domain radius is close to Ro at T_{upper}, the estimated maximum temperature for facile domain detection. Over a temperature range in which the amount of ordered bilayer is nearly constant, but domain size decreases as temperature increases, Fig. 6 *B* shows that the T_{mid} value, the midpoint for loss of domain detection is ~3Ro.

Based on this information, T_{mid} and T_{upper} values can be used to estimate domain sizes. As shown in Fig. 6 *C*, in 1:1:1 bSM/POPC/chol nanodomain radius gradually decreases

from ~150 Å near 10°C to 80–100 Å at 23°C to as small as <40 Å before melting at 45°C. Assuming a lipid cross-sectional area of ~70 $Å^2$, this gives the number of lipids in a circular domain decreasing from ~1000 lipids in one leaflet at 10°C to ~360 lipids at 23°C and <70 lipids at 45°C. Fig. 6 *C* also shows the estimated increase in domain size induced by the presence of TX-100. There is a several-fold increase in size. The size increase in the presence of LW peptide was somewhat smaller (not shown).

These domain radii values are only estimates. If domains are irregular they will have a larger circumference/area ratio than circular domains, and many more molecules near domain edges, leading to an underestimate of domain size. In addition, for the acceptor concentrations we used, which are not sufficient to totally quench fluorescence, calculations (not shown) suggest the domain radii may be overestimates by up to a factor of almost two.

DISCUSSION

Nanodomain size and the effect of TX-100 and transmembrane helices on domain formation and size

This study shows that nanodomain size in bSM/POPC/chol is strongly temperature dependent, decreasing as temperature increases. A temperature-dependent decrease in domain size is also predicted by the critical fluctuation model for nanodomains (26), and that similar nanodomain sizes have been proposed for other lipid mixtures (27). Our FRET data also show that in the presence of TX-100 or LW peptide domain size in bSM/POPC/chol vesicles increase significantly. Given the apparent T_{mid} for FRET for the NBD-rhodamine pair at 23°C when there is 4 mol % TX-100 in the membrane (samples with 150 μM total TX-100), domain radius must increase to 150 Å near room temperature based on the analysis above. An important question is how this size increase relates to prior work on the effect of TX-100 in SM/POPC/chol. It has been proposed that TX-100 binding to vesicles induces domain formation by reducing the miscibility of SM with molecules (unsaturated lipids and TX-100) concentrated within the Ld state (12,13). The analysis of the calorimetric studies on which this was based predicted that the T_{mid} temperature for domain separation in 1:1:1 SM/POPC/chol exhibits an increase from 20°C to ~35°C when the membranes contain 3 mol % TX-100 (13), and raw calorimetric data showed that a transition at 23°C was accompanied by an additional peak near 45°C as TX-100 concentration was increased from 0 to 3 or 7.7 mol % in these mixtures (12). This is the same range of TX-100 concentrations in the membrane that we investigated. (We also find that at a very high TX-100 concentration (1% v/v), solubilization versus temperature had a midpoint (50% solubilization) that was also close to 35°C (not shown).)

However, in contrast to conclusions from calorimetry, our studies find that the interaction of TX-100 with membranes does not increase the thermal stability of ordered domains, i.e., methods that can detect small nanodomains, such as nitroxide quenching show there are no temperatures at which the total fraction of the membrane in the form of ordered domains increases in the presence of TX-100. Instead, we find that TX-100 increases the size of individual domains by domain coalescence. This may not be inconsistent with calorimetric data. The melting of the small nanodomains might not be sufficiently cooperative in temperature, or might not involve a high enough enthalpy change, to have been detected by calorimetry. In fact, the idea that TX-100 induces phase separation may be formally correct if large domains can be considered phases while small nanodomains cannot be considered phases. Nevertheless, the key point is that the formation of nanodomains is not dependent upon TX-100. Because nanodomains are similar to the type of domains thought to form in plasma membranes, they are likely to be the most physiologically relevant species. In fact, experimentally the tendency of TX-100 to increase domain size may be a desirable property that allows the physical isolation of merged nanodomains as DRMs, even if the merger of small domains into large ones is an artifact.

The lack of domain formation by TX-100 is consistent with the overwhelming evidence that when there is preexisting domain formation, TX-100 solubilization reflects underlying domain behavior. In particular, it has been observed many times that when membranes have coexisting Lo and Ld domains before TX-100 addition, the Ld domains dissolve while the Lo domains are resistant to TX-100 solubilization (3,7–11). Studies also show that there is no expansion of preexisting Lo domains in supported bilayers (in which individual ordered domains cannot migrate and merge, and so individual domain size cannot increase) upon TX-100 addition (9–11), although such an expansion might be predicted if TX-100 reduced the miscibility of SM in the disordered domains. In fact, there is often partial solubilization of the Lo domains (9–11), consistent with the concept that the addition of TX-100 would lead to an *under*estimation of Lo domain formation (6). Furthermore, low concentrations of TX-100 tend to induce budding and fission of vesicles containing Lo domains from vesicles containing coexisting Lo and Ld domains (28), further enhancing the similarity between DRMs and the Lo domains from which they arise. Nevertheless, we are not arguing that DRMs are identical to preexisting rafts, and the isolation of DRMs from a cellular membrane, especially at 4°C, cannot be proof of the existence of preexisting rafts.

It is also interesting that the presence of a modest amount of transmembrane helices may be more effective than TX-100 at increasing domain size at cholesterol concentrations likely to exist in plasma membranes. This increases the probability of domain formation in natural membranes

and suggests that the effect of TX-100 in a protein-containing membrane is less than in a simple lipid bilayer.

An important question is why TX-100 increases domain size. One possibility comes from the molecular dynamics studies by P. Butler and colleagues showing that TX-100 decreases bilayer width (P. Butler, Penn State University, personal communication, 2011) in a fashion such that TX-100 would increase the mismatch in width between Ld and Lo domains, and thus increase line tension. An increase in domain size would minimize the amount of lipid at Lo/Ld boundaries and thus the unfavorable line tension energy.

SUPPORTING MATERIAL

Additional calculations and details, with three tables and 12 figures, are available at http://www.biophysj.org/biophysj/supplemental/S0006-3495(11)01186-6.

The authors thank Lindsay D. Nelson for preliminary studies on the effect of cholesterol on domains and Salvatore Chiantia for helpful discussions.

This research was supported by National Institutes of Health grant GM 48695 and National Science Foundation grant MCB 1019986.

REFERENCES

1. Simons, K., and G. van Meer. 1988. Lipid sorting in epithelial cells. *Biochemistry.* 27:6197–6202.
2. Brown, D. A., and J. K. Rose. 1992. Sorting of GPI-anchored proteins to glycolipid-enriched membrane subdomains during transport to the apical cell surface. *Cell.* 68:533–544.
3. Ahmed, S. N., D. A. Brown, and E. London. 1997. On the origin of sphingolipid/cholesterol-rich detergent-insoluble cell membranes: physiological concentrations of cholesterol and sphingolipid induce formation of a detergent-insoluble, liquid-ordered lipid phase in model membranes. *Biochemistry.* 36:10944–10953.
4. Schroeder, R., E. London, and D. Brown. 1994. Interactions between saturated acyl chains confer detergent resistance on lipids and glycosylphosphatidylinositol (GPI)-anchored proteins: GPI-anchored proteins in liposomes and cells show similar behavior. *Proc. Natl. Acad. Sci. USA.* 91:12130–12134.
5. Brown, D. A., and E. London. 2000. Structure and function of sphingolipid- and cholesterol-rich membrane rafts. *J. Biol. Chem.* 275:17221–17224.
6. London, E., and D. A. Brown. 2000. Insolubility of lipids in triton X-100: physical origin and relationship to sphingolipid/cholesterol membrane domains (rafts). *Biochim. Biophys. Acta.* 1508:182–195.
7. Dietrich, C., L. A. Bagatolli, …, E. Gratton. 2001. Lipid rafts reconstituted in model membranes. *Biophys. J.* 80:1417–1428.
8. Dietrich, C., Z. N. Volovyk, …, K. Jacobson. 2001. Partitioning of Thy-1, GM1, and cross-linked phospholipid analogs into lipid rafts reconstituted in supported model membrane monolayers. *Proc. Natl. Acad. Sci. USA.* 98:10642–10647.
9. El Kirat, K., and S. Morandat. 2007. Cholesterol modulation of membrane resistance to Triton X-100 explored by atomic force microscopy. *Biochim. Biophys. Acta.* 1768:2300–2309.
10. Morandat, S., and K. El Kirat. 2007. Real-time atomic force microscopy reveals cytochrome *c*-induced alterations in neutral lipid bilayers. *Langmuir.* 23:10929–10932.
11. Garner, A. E., D. A. Smith, and N. M. Hooper. 2008. Visualization of detergent solubilization of membranes: implications for the isolation of rafts. *Biophys. J.* 94:1326–1340.
12. Heerklotz, H. 2002. Triton promotes domain formation in lipid raft mixtures. *Biophys. J.* 83:2693–2701.
13. Heerklotz, H., H. Szadkowska, …, J. Seelig. 2003. The sensitivity of lipid domains to small perturbations demonstrated by the effect of Triton. *J. Mol. Biol.* 329:793–799.
14. Bakht, O., P. Pathak, and E. London. 2007. Effect of the structure of lipids favoring disordered domain formation on the stability of cholesterol-containing ordered domains (lipid rafts): identification of multiple raft-stabilization mechanisms. *Biophys. J.* 93:4307–4318.
15. Cheng, H. T., E. Megha, and, and London. 2009. Preparation and properties of asymmetric vesicles that mimic cell membranes: effect upon lipid raft formation and transmembrane helix orientation. *J. Biol. Chem.* 284:6079–6092.
16. Bakht, O., and E. London. 2007. Detecting ordered domain formation (lipid rafts) in model membranes using Tempo. *Methods Mol. Biol.* 398:29–40.
17. Kleemann, W., and H. M. McConnell. 1976. Interactions of proteins and cholesterol with lipids in bilayer membranes. *Biochim. Biophys. Acta.* 419:206–222.
18. Lentz, B. R., Y. Barenholz, and T. E. Thompson. 1976. Fluorescence depolarization studies of phase transitions and fluidity in phospholipid bilayers. 2 Two-component phosphatidylcholine liposomes. *Biochemistry.* 15:4529–4537.
19. Chattopadhyay, A., and E. London. 1984. Fluorimetric determination of critical micelle concentration avoiding interference from detergent charge. *Anal. Biochem.* 139:408–412.
20. Fastenberg, M. E., H. Shogomori, …, E. London. 2003. Exclusion of a transmembrane-type peptide from ordered-lipid domains (rafts) detected by fluorescence quenching: extension of quenching analysis to account for the effects of domain size and domain boundaries. *Biochemistry.* 42:12376–12390.
21. Wenz, J. J., and F. J. Barrantes. 2003. Steroid structural requirements for stabilizing or disrupting lipid domains. *Biochemistry.* 42:14267–14276.
22. Alanko, S. M., K. K. Halling, …, B. Ramstedt. 2005. Displacement of sterols from sterol/sphingomyelin domains in fluid bilayer membranes by competing molecules. *Biochim. Biophys. Acta.* 1715:111–121.
23. Chattopadhyay, A., and E. London. 1987. Parallax method for direct measurement of membrane penetration depth utilizing fluorescence quenching by spin-labeled phospholipids. *Biochemistry.* 26:39–45.
24. Ayuyan, A. G., and F. S. Cohen. 2008. Raft composition at physiological temperature and pH in the absence of detergents. *Biophys. J.* 94:2654–2666.
25. Silvius, J. R. 2003. Fluorescence energy transfer reveals microdomain formation at physiological temperatures in lipid mixtures modeling the outer leaflet of the plasma membrane. *Biophys. J.* 85:1034–1045.
26. Honerkamp-Smith, A. R., P. Cicuta, …, S. L. Keller. 2008. Line tensions, correlation lengths, and critical exponents in lipid membranes near critical points. *Biophys. J.* 95:236–246.
27. Heberle, F. A., J. Wu, …, G. W. Feigenson. 2010. Comparison of three ternary lipid bilayer mixtures: FRET and ESR reveal nanodomains. *Biophys. J.* 99:3309–3318.
28. Staneva, G., M. Seigneuret, …, M. I. Angelova. 2005. Detergents induce raft-like domains budding and fission from giant unilamellar heterogeneous vesicles: a direct microscopy observation. *Chem. Phys. Lipids.* 136:55–66.